prediction of engine cooling fan noise radiation

by Sean F. Wu

Professor, Director, Acoustics, Vibration, and Noise Control Laboratory, Department of Mechanical Engineering, Wayne State University, Detroit, MI 48202

A semi-analytic and semi-empirical formula is developed for predicting noise radiation from engine cooling fan assemblies. In this formula, the tonal sounds centered at the BPF (blade passage frequency) and its harmonics of the fan are determined by solving fluctuating forces exerted on the surrounding fluid medium by rotating blades, and the narrow and broad band sounds are described by normal distribution-like functions. The effects of shroud, upstream radiator/condenser set, and downstream engine block are approximated by shape functions. The computer model thus obtained is used to calculate the noise spectra from different fan assemblies under various working conditions and validated against the measured data. This model is used to predict the overall sound pressure levels from dimensionally similar fans running under different working conditions, and the results are compared with those estimated by the fan laws currently in use by engineers in the automotive industry.

Introduction

Reduction of engine cooling fan noises has become an increasingly urgent task in the automotive industry as the requirements for passenger compartment comfort increase, and as other vehicle components such as the engine, powertrain, exhaust system, etc. are made quieter. To reduce fan noise cost-effectively, it is necessary to incorporate the component of noise reduction into an early design stage. To this end, we must have a computer model that will allow design engineers to simulate noise radiation from an engine cooling fan assembly, given its characteristic design parameters and working conditions.

For most US passenger vehicles, the engine cooling fan is installed inside a shroud with a radiator/condenser set placed in the upstream (known as the "pull-in" type fan), and an engine block in the downstream. The shroud is designed to guide the ingested airflow and to provide certain protection for the mechanics in inspecting an engine compartment under an operating condition. Because of the compactness of an engine compartment, the shroud extension covers are often made asymmetric. As a result, the ingested airflow is greatly distorted and a significant amount of unsteady fluctuating forces are generated. These unsteady fluctuating forces are much more effective in generating aerodynamic sounds than the steady fluctuating forces. Experimental results demonstrate that the presence of a shroud can increase the levels of discrete sounds centered at the BPF and its harmonics by 10 – 17 dB(A) [Wu et al., 1998].

When a radiator/condenser set is placed in the upstream of a fan/shroud assembly, the ingested airflow becomes not only asymmetric, but also turbulent after passing through many tiny irregularly-shaped slots built in the radiator and condenser. Experimental results show that intake turbulence tends to reduce the coherence of the unsteady fluctuating forces generated by a shroud, thus reducing its effectiveness in generating the discrete sounds. On the other hand, it increases the levels of the broadband sounds. Consequently, the levels of the discrete sounds are lowered slightly but their bandwidths are widened.

The flow field generated by this fan/shroud/radiator/condenser assembly is further complicated by an engine block situated in the downstream. The compactness of an engine compartment forces the discharged airflow to re-circulate to the intake of the fan assembly, making it possible to generate the so-called "chopping" sounds. More importantly, this compactness raises the static pressure drop across the fan assembly, which has a direct impact on the resulting flow rate. Experimental results show that for a fixed power input, an increase in the static pressure drop reduces the fan speed and the overall flow rate, thus impairing its cooling performance. However, measurement data also indicate that the increase in the static pressure drop across a fan assembly has little impact on the overall noise spectra.

Obviously, it is unrealistic to attempt to model the entire flow field surrounding an engine cooling fan assembly as described above. Hence analytic solutions cannot be obtained even with the use of the most sophisticated computers to date. Yet, estimations of the noise spectra from an engine cooling fan assembly are desired, especially in an early design stage to reduce resulting noise radiation in a cost-effective manner.

In what follows, we present an engineering computer model for estimating noise spectra of an engine cooling fan assembly. Figure 1 illustrates the corresponding computer flow chart. In this model, the effects of the unsteady fluctuating forces on discrete sounds generated by a shroud, the intake turbulence on broadband sounds produced by radiator and condenser, and the static pressure changes caused by the compactness of an engine compartment are approximated by certain shape functions.

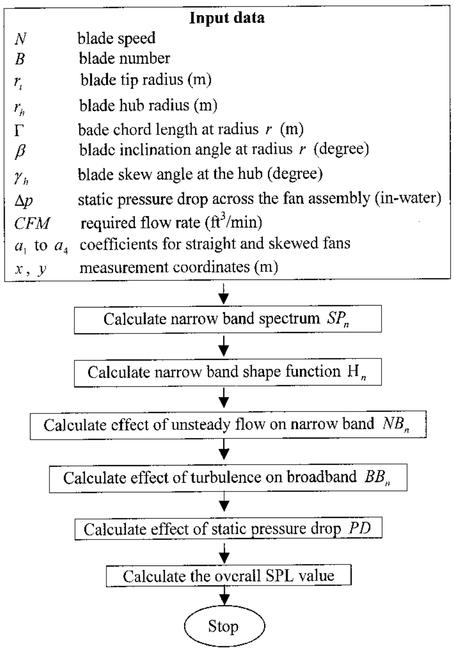

Figure 1. Flow chart for calculating noise spectrum of an engine cooling fan assembly

Formulations

The semi-analytic and semi-empirical formula for describing the noise spectrum from an engine cooling fan assembly can be written as follows

$$sp = \sum_{n=0}^{\infty} PD(NB_n + BB_n)\mathrm{Re}\left[SP_n \mathrm{H}_n(f)^{-i2\pi nBf_0 t}\right], \qquad (1)$$

where PD depicts the effect of static pressure drop across the fan assembly induced by an engine compartment

$$PD = 10^{0.15(\Delta p + 0.19)}, \qquad (2)$$

where Δ_p is the static pressure drop across the fan assembly (in-water), which is prescribed by the pressure-flow characteristic curve of a fan. The symbols NB_n and BB_n in Eq. (1) account for the effect of the unsteady fluctuating forces generated by a shroud on the narrow band sounds centered at the BPF and its harmonics, and that of incident turbulence induced by an upstream radiator/condenser set on the broadband sounds, respectively,

$$NB_n = a_1\left[1 + a_2\left(\frac{f_n}{f_0}\right)\right]^{-1}, \text{ and } BB_n = a_3\left[1 + a_4\left(\frac{f_n}{f_0}\right)\right]^{-1}, \qquad (3)$$

where the parameters a_i, $i =$ 1 to 4, depend on the designs of the shroud, radiator, and condenser. In this case, they are determined by curve fitting experimental data for all fan assemblies subject to various working conditions (see Table 1).

Table 1. Values of coefficients a_i for straight and back-skewed blades.

a_i	Straight blade Fan with Shroud	Skewed blade Fan with shroud and radiator/ condenser	Fan with shroud	Fan with shroud and radiator/ condenser
a_1	4.600	3.10	4.35	4.35
a_2	6.600	5.10	5.80	11.00
a_3	0.450	1.00	0.34	0.50
a_4	0.093	0.93	0.16	0.40

The function SP_n Eq. (1) represents the amplitude of the nth narrow band of the noise spectrum

$$SP_n = \int_{r_h}^{r_t} \frac{27.4\rho C_L \Gamma V_0^2 B^2 \left[0.96739(1-\xi_b)-0.2924\right]\cos\psi \sin\theta \sin(\psi-\beta)}{16\pi^2 R_0 \left[1-0.0217(1-\xi_b)(f/f_0)\sin(\gamma_h-\gamma)\right]} \times \left(1-e^{-54.8\pi r/B}\right)\left(i\frac{2\pi nBf_0}{c}-\frac{1}{R_0}\right)\frac{(2-\delta_{0n})e^{i2\pi nBf_0\sqrt{R_0^2+r^2}/c}}{(27.4r)^2+(nB)^2} r\,dr, \quad (4)$$

and H_n in Eq. (1) is the shape function for the nth narrow band whose amplitude is unity at the center frequency of the band, but decays exponentially as the frequency deviates from the center frequency

$$\mathrm{H}_n(f) = \left(1-\left|\frac{f-nf_0}{f_0}\right|\right) H\left[f-(n-1)f_0\right] H\left[(n+1)f_0-f\right] e^{-\left(\frac{f-nf_0}{f_0\sigma_n}\right)^2}, \quad (5)$$

where H represents the Heaviside step function and $\sigma_n = n/5$ indicates the decay rate of the nth narrow band.

In Eq. (4) C_L is the lift coefficient defined by Pao [1967],

$$C_L = 5.73\sin(\psi-\beta), \quad (6)$$

where H is the blade inclination angle at radius r, and ψ is given by

$$\psi = \tan^{-1}\left(\frac{\kappa}{r}\right), \quad (7)$$

where

$$\kappa = \frac{CFM}{2\pi^2 f\left(r_t^2-r_h^2\right)}, \quad (8)$$

where CFM represents the required flow rate (ft^3/min), r_t and r_h are the tip and hub radii of the fan blade, respectively. The quantity V_0^2 in Eq. (4) is the mean-squared flow velocity $V_0^2 = 4\pi^2 f^2(r^2+\kappa^2)$, and the symbol ξ is the solidity of the blade disk area

$$\xi_b = \frac{B}{\pi\left(r_t^2-r_h^2\right)}\int_{r_h}^{r_t} \Gamma\cos\beta\, dr, \quad (9)$$

where B is the number of blades and Γ is the blade chord length at radius r. The quantities $\theta = \tan^{-1}(y/x)$ and $R_0 = \sqrt{x^2+y^2}$ represent the polar coordinates of the measurement point, with x and y being the horizontal and vertical distances measured with respect to the center of the fan disk. The quantity γ_h and γ in Eq. (4) are the blade skew angles at the hub r_h and at radius r, respectively, ρ is the density of the fluid medium, d_{ij} is the Kronecker delta, $f_0 = NB/60$ is the BPF, and N is the fan speed.

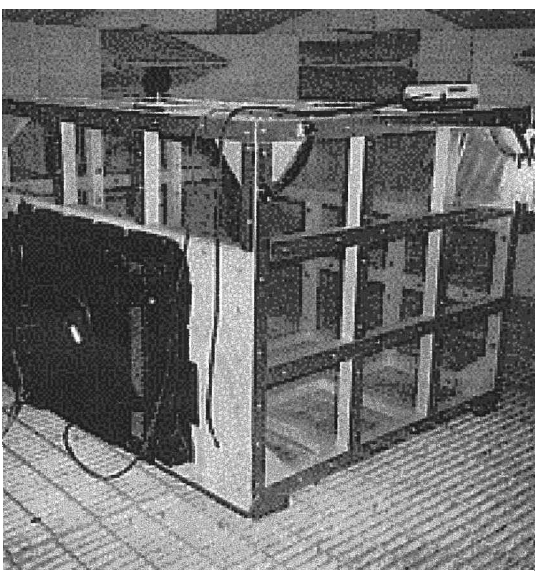

Figure 2. Setup for an engine cooling fan assembly mounted on a test plenum.

Test Setup

To validate Eq. (1), a test plenum was built (see Figure 2), which was made of a wood-framed box covered by Mylar sheets. This plenum was designed to simulate the static pressure drop across a fan assembly installed in an engine compartment of a full-size vehicle. In the experiments the airflow was drawn into the box through an adjustable door across the fan assembly and discharged directly to the outside. The desired static pressure drops were obtained by adjusting the opening of the doorway and monitored by a digital barometer. The fan was driven by an HP DC power supplier and the fan speed monitored by a laser speedometer. Since Mylar was transparent to sound wave but impermeable to airflow, it had a minimum effect on the fan noises.

The noise signals radiated from the fan assembly were measured by a B&K Prepolarized Free-field Condenser Microphone Type 4189 at both upstream and downstream positions, and were analyzed by a B&K Dual Channel Analyzer Type 2032. The data acquisition and processing were controlled by an IBM PC computer using the StarAcoustics® software. The experiments were conducted in a walk-in size, fully anechoic chamber in the Acoustics, Vibration, and Noise Control (AVNC) Laboratory at Wayne State University.

Figure 3. Test setup for Type A fan alone.

Results and discussions

In this section we present validation results from two completely different fan assemblies termed as Types A and B for proprietary reasons. These fans were tested with shrouds and with shrouds and radiator/condenser sets, respectively. Since the cooling fans were designed to run at low- and high-speed regimes (one for idle and the other for cruising at high speeds), validations were done in both speed regimes.

In each test, the noise spectra were measured at the same distance, namely, $x = 2$ m and $y = 0.5$ m with respect to the center of the fan disk. These measured spectra were compared with the calculated ones under the same conditions. For brevity, however, only two comparisons were shown for each fan assembly, one in the low- and the other in the high-speed regimes.

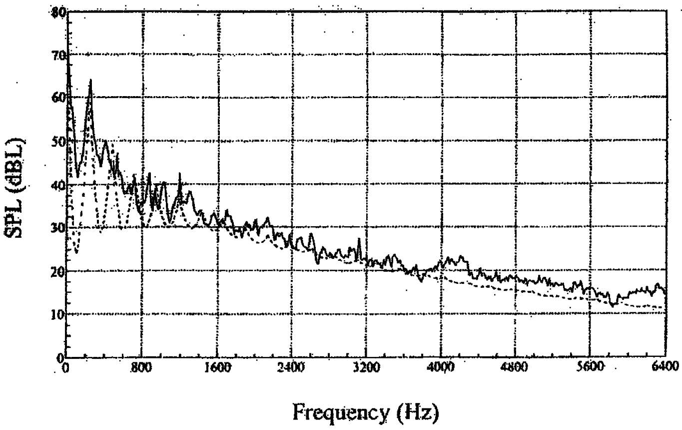

Figure 4. Comparison of noise spectra from Type A fan with shroud running in the low-speed regime. Solid line: Measured; Dashed line: Calculated.

Type A fan

This was a production fan used in a four-door sedan with nine back-skewed blades (see Figure 3). Figure 4 depicts the comparison of the calculated and measured noise spectra from Type A fan with a shroud running in the low-speed regime at 1,584 rpm. The corresponding flow rate and static pressure drop were 1,105 CFM and 0.309 in-water, respectively. Figure 5 demonstrates the comparison of noise spectra from the same fan/shroud assembly running in the high-speed regime at 2,052 rpm, with a flow rate of 2,034 CFM and a static pressure of 0.495 in-water. Table 2 summarizes the SPL values of the first two discrete sounds and those of the overall sounds. Results show that the present computer model captured the main characteristics of Type A fan noise spectra.

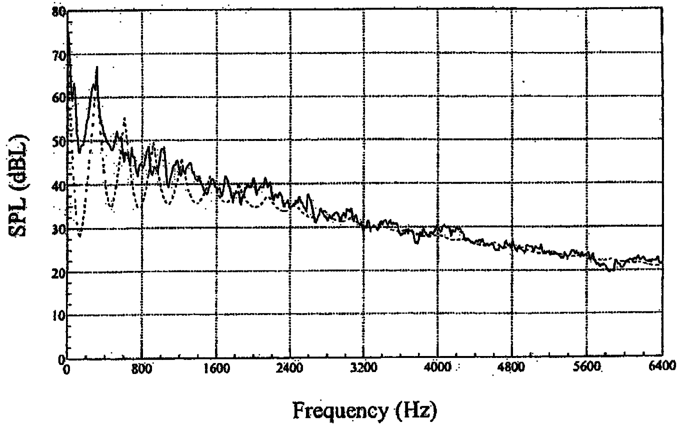

Figure 5: Comparison of noise spectra from Type A fan with shroud running in the high-speed regime. Solid line: Measured; Dashed line: Calculated.

	Frequency	Measured	Calculated	Difference	Speed
(Hz)	SPL	(dB) SPL	(dB)	SPL (dB)	Regime (rmp)
Peak No. 1	237.6	64.1	59.3	-4.8	1584 (low)
Peak No. 2	475.2	50.3	49.7	-0.6	1584 (low)
Total SPL (dBA)	**0 to 6,400**	**62.2**	**59.7**	**-2.5**	**1584 (low)**
Peak No. 1	307.8	67.3	65.4	-1.9	2052 (high)
Peak No. 2	615.6	50.5	55.9	+5.4	2052 (high)
Total SPL (dBA)	**0 to 6,400**	**68.7**	**68.3**	**-0.4**	**2052 (high)**

Table 2. Comparison of SPL values of the first two discrete and overall sounds for Type A fan with shroud in both low- and high-speed regimes.

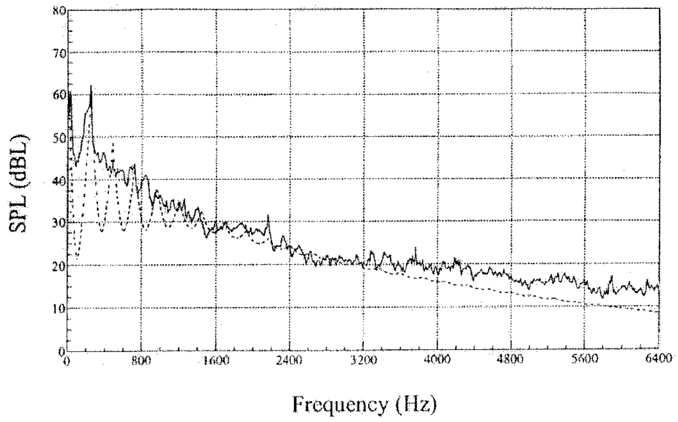

Figure 6. Comparison of noise spectra from Type A fan with shroud/radiator/condenser running in the low-speed regime. Solid line: Measured; Dashed line: Calculated.

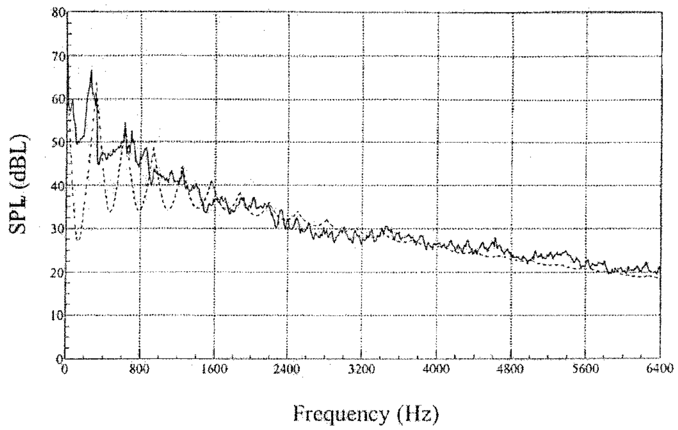

Figure 7. Comparison of noise spectra from Type A fan with shroud/radiator/condenser running in the high-speed regime. Solid line: Measured; Dashed line: Calculated.

Figures 6 and 7 display the comparisons of the calculated noise spectra with those measured from Type A fan with shroud/radiator/condenser assembly running in both low- and high-speed regimes. In this case, the flow rate and static pressure drop for the low speed at 1,600 rpm were 1,650 CFM and 0.114 in-water, respectively, and those for the high speed at 2,088 rpm were 2,108 CFM and 0.478 in-water, respectively. Once again, the calculated noise spectra and overall SPL values agreed well with the measured ones. The differences in the calculated and measured SPL values for the first two discrete sounds ad those of the overall sounds are listed in Table 3.

Table 3. Comparison of SPL values of the first two discrete and overall sounds for Type A fan with shroud/radiator/condenser in both low- and high-speed regimes.

	Frequency (Hz)	Measured SPL (dB)	Calculated SPL (dB)	Difference SPL (dB)	Speed Regime (rmp)
Peak No. 1	240.0	62.3	58.6	-3.7	1,600 (low)
Peak No. 2	480.0	44.0	49.1	+5.1	1,600 (low)
Total SPL (dBA)	**0 to 6,400**	**60.4**	**59.0**	**-1.4**	**1,600 (low)**
Peak No. 1	313.2	66.8	64.4	-2.4	2,088 (high)
Peak No. 2	626.4	54.2	54.9	+0.7	2,088 (high)
Total SPL (dBA)	**0 to 6,400**	**67.4**	**67.4**	**0.0**	**2,088 (high)**

Table 4. Comparison of SPL values of the first two discrete and overall sounds for Type B fan with shroud in both low- and high-speed regimes.

	Frequency (Hz)	Measured SPL (dB)	Calculated SPL (dB)	Difference SPL (dB)	Speed Regime (rmp)
Peak No. 1	211.7	59.9	59.3	-0.6	1,411 (low)
Peak No. 2	423.3	48.9	50.3	+1.4	1,411 (low)
Total SPL (dBA)	**0 to 6,400**	**60.5**	**59.6**	**-0.9**	**1,411 (low)**
Peak No. 1	305.9	67.1	69.1	+2.0	2,039 (high)
Peak No. 2	611.7	58.2	60.1	+1.9	2,039 (high)
Total SPL (dBA)	**0 to 6,400**	**71.9**	**72.8**	**+0.9**	**2,039 (high)**

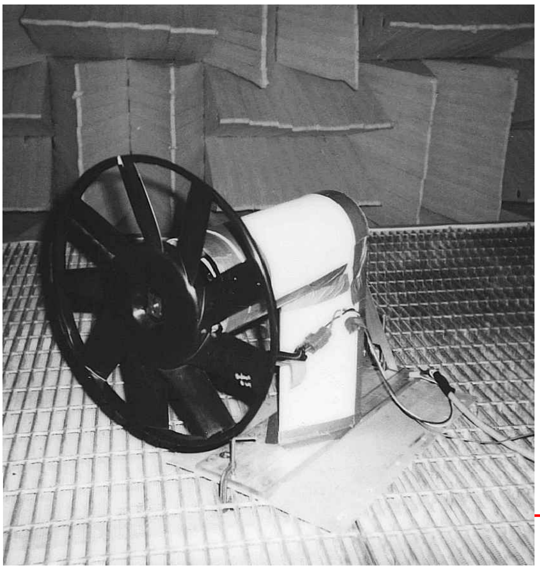

Type B Fan

Type B fan was a production fan used in a mini-van with nine straight blades (see Figure 8). Using the company supplied blade geometry and dimensions, we calculated the spectra from Type B fan with a shroud running at both low and high speeds. The flow rate and static pressure drop at 1,411 rpm (low-speed regime) were 635 CFM and 0.438 in-water, respectively, and those at 2,039 rpm

Figure 8. Test setup for Type B fan alone.

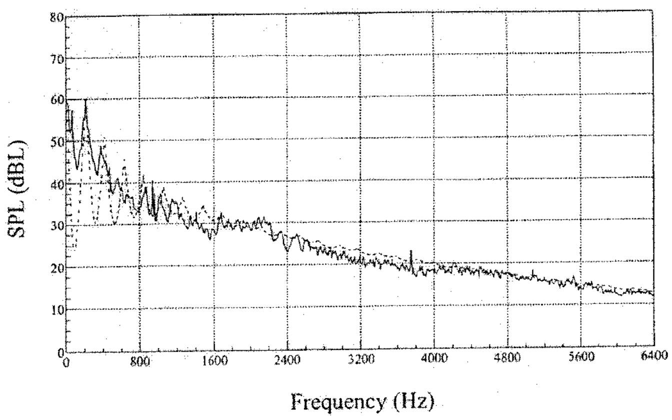

Figure 9. Comparison of noise spectra from Type B fan with shroud running in the low-regime. Solid line: Measured; Dashed line: Calculated.

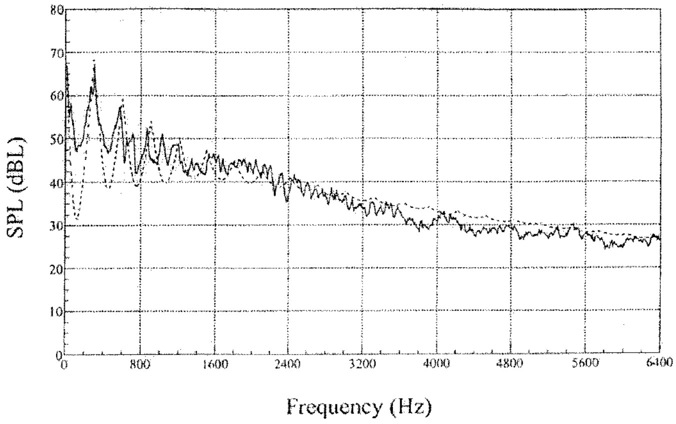

Figure 10. Comparison of noise spectra from Type B fan with shroud running in the high-speed regime. Solid line: Measured; Dashed line: Calculated.

(high-speed regime) were 1,890 CFM and 0.358 in-water, respectively. The corresponding comparisons of the calculated and measured noise spectra are shown in Figures 9 and 10, and the differences between the calculated and measured SPL values for the first two discrete sounds and the overall sounds were summarized in Table 4.

Figures 11 and 12 illustrate the comparisons of the calculated and measured noise spectra from Type B fan with a shroud and radiator/condenser assembly running at both low and high speeds, respectively. In this case, the flow rate and static pressure drop at a low speed of 1,425 rpm were 1,155 CFM and 0.282 in-water, respectively, and those for at a high speed of 1,997 rpm were 1,750 CFM and 0.439 in-water, respectively. Table 5 illustrates the differences between the calculated and measured SPL values for the first two discrete sounds and the overall sounds.

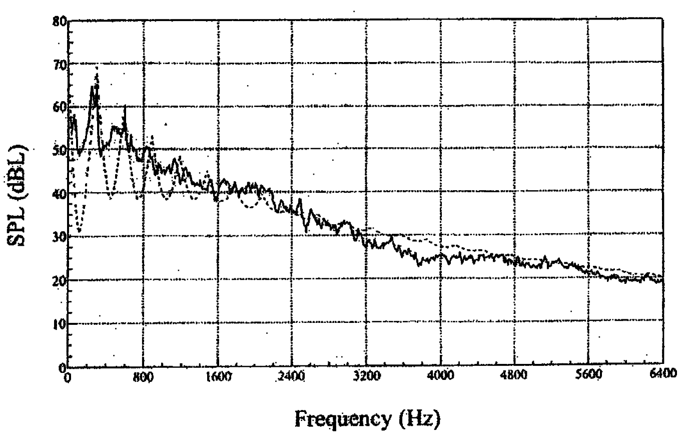

Figure 12. Comparison of noise spectra from Type B fan with shroud/radiator/condenser running in the high-speed regime. Solid line: Measured; Dashed line: Calculated.

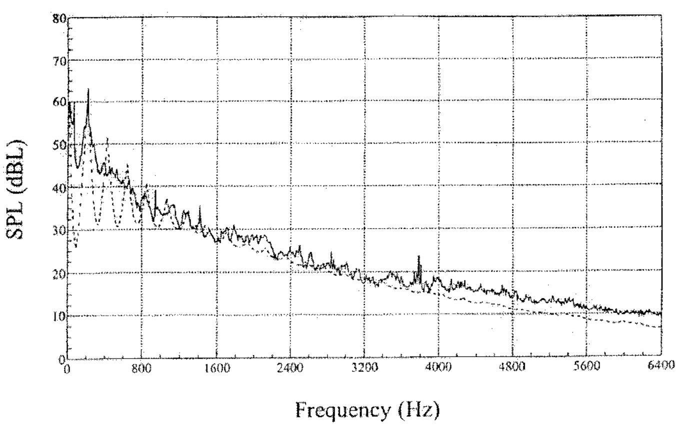

Figure 11. Comparison of noise spectra from Type B fan with shroud/radiator/condenser running in the low-speed regime. Solid line: Measured; Dashed line: Calculated.

Table 5. Comparison of SPL values of the first two discrete and overall sounds for Type B fan with shroud/radiator/condenser in both low- and high-speed regimes.

	Frequency (Hz)	Measured SPL (dB)	Calculated SPL (dB)	Difference SPL (dB)	Speed Regime (rmp)
Peak No. 1	213.8	63.0	60.0	-3.0	1,425 (low)
Peak No. 2	427.5	45.0	51.0	+7.0	1,425 (low)
Total SPL (dBA)	**0 to 6,400**	**61.3**	**60.4**	**-0.9**	**1,425 (low)**
Peak No. 1	299.6	65.3	68.3	+3.0	1,997 (high)
Peak No. 2	626.4	60.3	59.3	-1.0	1,997 (high)
Total SPL (dBA)	**0 to 6,400**	**71.4**	**71.8**	**+0.4**	**1,997 (high)**

Results demonstrate that good agreements were obtained in all cases for Type B fan. The agreements between the calculated and measured spectra were actually better than those of Type A fan. In particular, the differences between the calculated and measured total SPL values were less than 1 dB. The reason could be due to the fact that the skewed blades of Type A fan had generated more turbulence than the straight blades of Type B fan, and these turbulence effects were not considered in the computer model.

Virtual Design of Engine Cooling Fan

Equation (1) allows one to assess the performance of an engine cooling fan assembly, given its characteristic dimensions and working conditions. It also provides guidelines for an engineer to explore various alternatives in the design of an engine cooling fan to meet cooling, noise, and space requirements before the fan is actually fabricated. In particular, this formulation enables one to examine the effects of blade number, inclination angle, skew angle, chord length, diameter, speed, flow rate, and static pressure drop on discrete tonal and broadband sounds, as well as the overall sound pressure level in both A-weighting and linear scales. On the other hand, the fan laws currently in use by the practicing engineers can only provide the changes in the overall SPL values in the linear scale for dimensionally similar fans due to changes in diameter, speed, flow rate, and static pressure drop.

As an example, let us consider Type A fan with a diameter $D_2 = 388$ mm, flow rate $Q_2 = 1{,}300$ ft^3/min, speed $N_2 = 2{,}185$ rpm, and static pressure $P_2 = 0.69$ in-water. Suppose that we decide to increase the flow rate to $Q_1 = 1{,}400$ ft^3/min, while keeping the fan dimension constant. From the fan laws, we find that in order to deliver a higher flow rate the fan speed must increase to

$$N_1 = N_2\left(\frac{Q_1}{Q_2}\right)\left(\frac{D_2}{D_1}\right)^3 = 2{,}185\left(\frac{1{,}400}{1{,}300}\right)\left(\frac{388}{388}\right)^3 = 2{,}353\ \text{rpm}. \qquad (10)$$

The static pressure drop will change accordingly to

$$P_1 = P_2\left(\frac{D_1}{D_2}\right)^2\left(\frac{N_1}{N_2}\right)^2 = 0.69\left(\frac{388}{388}\right)^2\left(\frac{2{,}353}{2{,}185}\right)^2 = 0.80\ \text{in-water.} \qquad (11)$$

Once $D_{1,2}$ and $N_{1,2}$, or $D_{1,2}$ and $P_{1,2}$ are specified, the change in the total SPL value can be estimated as,

$$\Delta SPL = 20\log_{10}\left(\frac{D_1}{D_2}\right)^{3.5} + 20\log_{10}\left(\frac{N_1}{N_2}\right)^{2.5} = 20\log_{10}\left(\frac{2{,}353}{2{,}185}\right)^{2.5} = 1.6\ \text{(dBL);} \qquad (12a)$$

or

$$\Delta SPL = 20\log_{10}\left(\frac{D_1}{D_2}\right) + 20\log_{10}\left(\frac{P_1}{P_2}\right)^{1.25} = 20\log_{10}\left(\frac{0.80}{0.69}\right)^{1.25} = 1.6\ \text{(dBL).} \qquad (12b)$$

However, using Eq. (1) one can plot the entire spectrum and examine its change as the flow rate increases from Q_2 to Q_1. In this case, the overall SPL values are found to increase from 81.4 dBL to 83.0 dBL, a net increase of 1.6 dBL, which agrees perfectly with the results of the fan laws.

Table 6 summarizes the examinations of the effects of changing blade diameter D_1, flow rate Q_1, speed N_1, and static pressure drop P_1 on the changes in the BPF and total SPL values of Type A fan by using Eq. (1). The results thus obtained are then compared with those of the fan laws (see the last column of Table 6).

Similar virtual designs for Type B fan can be conducted and the effects of changing blade diameter, flow rate, speed, and static pressure drop on the BPF and overall SPL values can be obtained by using Eq. (1) (see Table 7). Results show that good agreements between Eq. (1) and the fan laws are obtained in all cases.

	D	Q	N	P	BPF	Total	Total	DSPL	Fan
mm	ft3/m	rpm	in-water	(dBL)	(dBA)	(dBL)	(dBL)	Laws	
Test	388	1,300	2,186	0.69	71.2	74.6	81.4	0	0
Design	388	1,400	2,353	0.80	72.8	76.9	83.0	+1.6	+1.6
Design	388	1,500	2,521	0.92	74.2	79.0	84.5	+3.1	+3.1
Design	388	1,600	2,689	1.10	75.5	80.8	85.9	+4.5	+4.5
Test	420	1,300	1,723	0.50	72.7	73.9	82.0	0	0
Design	420	1,400	1,855	0.58	74.4	76.3	83.9	+1.8	+1.6
Design	420	1,500	1,988	0.67	77.8	80.4	87.7	+5.7	+3.1
Design	420	1,600	2,120	0.76	77.	80.5	87.0	+4.9	+4.5
Test	450	1,300	1,401	0.38	72.7	71.9	81.	0	0
Design	450	1,400	1,508	0.44	74.4	74.3	83.0	+1.8	+1.6
Design	450	1,500	1,616	0.51	76.0	76.6	84.7	+3.5	+3.1
Design	450	1,600	1.724	0.58	77.4	78.7	86.3	+5.1	+4.5
Test	500	1,300	1,021	0.25	688	64.7	75.9	0	0
Design	500	1,400	1,100	0.29	70.5	67.2	77.9	+2.1	+1.6
Design	500	1,500	1,178	0.33	72.1	69.6	79.6	+3.7	+3.1
Design	500	1,600	1,257	0.38	71.8	71.8	81.3	+4.5	+4.5

Table 6. Effects of design parameters of Type A fan on resulting noise levels.

	D	Q	N	P	BPF	Total	Total	DSPL	Fan
mm	ft3/m	rpm	in-water	(dBL)	(dBA)	(dBL)	(dBL)	Laws	
Test	418	1,550	1,990	0.48	73.4	76.9	82.4	0	0
Design	418	1,650	2,118	0.54	74.8	78.8	84.0	+1.6	+1.4
Design	418	1,750	2,247	0.61	76.2	80.7	85.4	+3.0	+2.6
Design	418	1,850	2,375	0.68	77.4	82.4	86.8	+4.4	+3.8
Test	450	1,550	1,595	0.36	71.9	73.2	80.1	0	0
Design	450	1,650	1,698	0.41	73.4	75.4	81.7	+1.6	+1.4
Design	450	1,750	1,801	0.46	74.7	77.3	83.2	+3.1	+2.6
Design	450	1,850	1,904	0.51	76.0	79.1	84.6	+4.5	+3.8
Test	480	1,550	1,314	0.28	69.6	69.3	77.1	0	0
Design	480	1,650	1,399	0.31	71.1	71.4	78.6	+1.6	+1.4
Design	480	1,750	1,484	0.35	72.4	73.3	80.3	+3.2	+2.6
Design	480	1,850	1,569	0.39	73.8	75.2	81.7	+4.6	+3.8
Test	510	1,550	1,096	0.22	67.4	65.4	74.1	0	0
Design	510	1,650	1,166	0.25	68.9	67.4	75.8	+1.7	+1.4
Design	510	1,750	1,237	0.28	70.3	69.5	77.2	+3.2	+2.6
Design	510	1,850	1,308	0.31	71.7	71.4	78.8	+4.7	+3.8

Table 7. Effects of design parameters of Type B fan on resulting noise levels.

87% of complaints noise-related

In New York, figures from the 'quality of life' hotline, manned by the police department, showed that there were 38,167 complaints received between January 1 and September 11 in there year 2000. Of those, 87% were noise-related. The next most popular subjects were animals and graffiti. Last year, 77% of complaints were noise-related.

Conclusions

A computer model for predicting noise spectrum of an engine cooling fan assembly is developed. The effects of fan shroud, radiator, condenser, and engine compartment on the resulting narrow and broad band sounds are considered. The computer model thus obtained is validated experimentally with two completely different fan assemblies. The calculated noise spectra compare well with the measured data under the same working conditions. Unlike the fan laws that can only estimate the changes in the overall SPL values in linear scale, this computer model can predict changes in the noise spectra, including the overall SPL values in both linear and A-weighting scales due to changes in blade geometry, dimension, and working conditions. While the present model can capture the main characteristics of cooling fan noise spectra, it is still not generalized for any type of fan assemblies because many coefficients such as a_i, $i = 1$ to 4, are fixed as constants. In order to generalize this computer model these coefficients must be correlated to the design parameters of the shroud, radiator, condenser, and engine compartment.

References

S. F. Wu S. G. Su, and H. S. Shah, Noise radiation from engine cooling fans, Journal of Sound and Vibration, Vol. 216, No. 1 107 – 132 1998.

R. H. F. Pao, Fluid Mechanics. Charles E. Merrill Books. 256 – 262 1967.